

## Introduction

The 2002-2003 Etna eruption offers a good case study to gain insight into the complex interaction between magma intrusive events and tectonic response because of: (i) the high-quality ground deformation data whose inversion allowed for a detailed description of the intrusive sources; (ii) the associated seismic activity recorded in the period spanning the intrusion. During the night of 26-27 October 2002, the opening of two eruptive fractures system on both the NE and S flanks of Etna volcano was accompanied and followed by an intense seismic sequence mainly affecting the volcano's eastern sector. Most of the earthquakes during the first hour took place in the central upper part of Mt Etna, and after mid-night migrated in the northeast direction involving the North East Rift and Pernicana Fault. In the following hours the eruptive fracture system opened on the north-eastern flank, nearly to the NERift. Geodetic data have been already inverted to imagine the observed deformation pattern. The inversion of tilt data and GPS horizontal and vertical components, recorded in the time interval 26-27 October spanning the eruption onset, required a vertical uprising dike in the southern flank and a lateral intrusion propagating along the north-eastern sector.

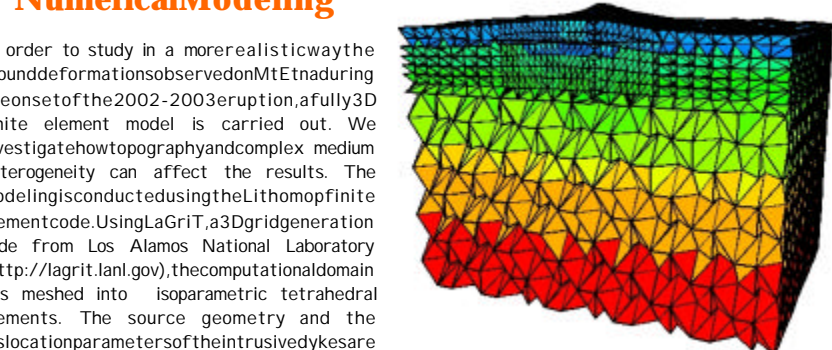
## Numerical Modeling

In order to study in a more realistic way the ground deformations observed on Mt Etna during the onset of the 2002-2003 eruption, a fully 3D finite element model is carried out. We investigate how topography and complex medium heterogeneity can affect the results. The modeling is conducted using the Lithoprobe finite element code from Los Alamos National Laboratory (<http://lagrit.lanl.gov>), the computational domain was meshed into isoparametric tetrahedral elements. The source geometry and the dislocation parameters of the intrusive dykes are based on the results of geodetic data inversion. In order to simulate the wedge-like intrusions we assigned dislocation boundary conditions implemented using "split nodes" to the nodes lying on the dykes surfaces.

The elastic parameters were estimated using  $V_p$  and  $V_s$  wave velocities inferred from seismic tomography. The subsurface elastic heterogeneities of the medium were included in the numerical model by assigning to each element in the meshed domain the value of the elastic Young's modulus interpolated at the element location. A Poisson ratio equal to 0.25 is assumed that is a reasonable approximation on Mt. Etna. In such a case, the Young's modulus,  $E$ , is related to medium density  $\rho$  and seismic wave velocity  $V_p$  through the following relation:

$$E = \frac{5}{6} \rho V_p^2$$

Using a medium density of  $2400 \text{ kg/m}^3$  the Young modulus varies in the range from  $11.5 \text{ GPa}$  at shallow depth to  $133 \text{ GPa}$  at higher depth.

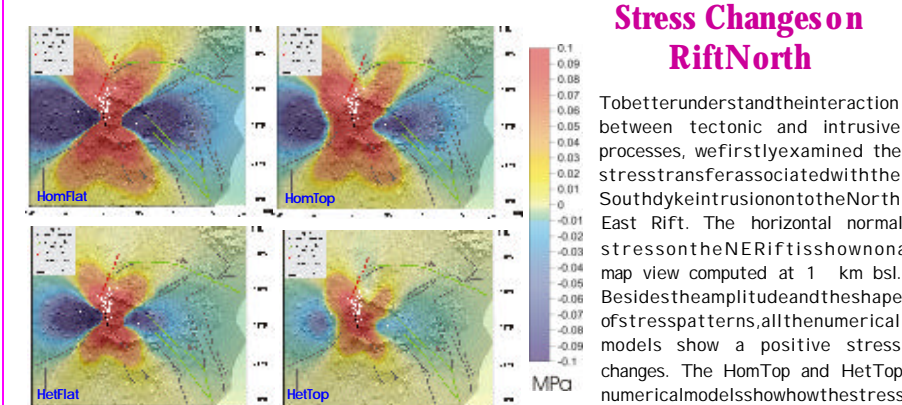
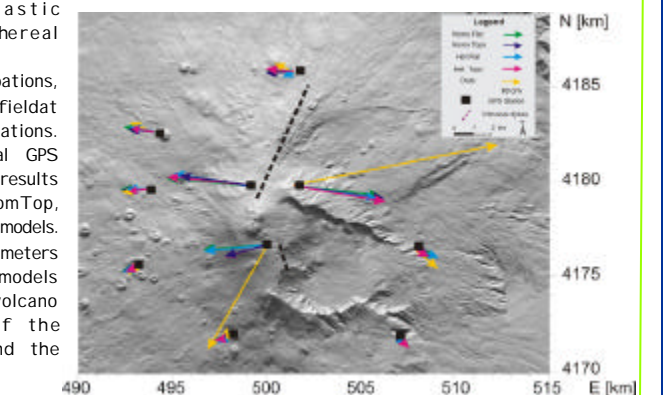


	Rift South	Rift North
X center [m]	499538.4	500682.1
Y center [m]	4175474.0	4181637.0
Depth [km]	2	0
Length [km]	1.5	7.8
Width [km]	1.6	3.1
Azimuth [°]	-17.2	23.3
Dip [°]	80.3	81.9
Strike Slip [m]	0.0	1.0
Dip Slip [m]	0.0	0.0
Opening [m]	1.5	1.0

## Ground Deformation

Discrepancies with respect to the analytical results are expected on ground deformation values predicted by the numerical models because of the medium heterogeneity and the irregular topography of Mt Etna. Indeed, the volcano edifice is rather asymmetric having a prominent mass deficit in the eastern sector with respect to the western sector in correspondence of Valle del Bove. A good approach to estimate how material properties and topography may affect the ground deformation is to evaluate each one separately and compare the results. Therefore, we conduct four numerical models in which we considered: (i) an homogeneous elastic medium with a flat surface (HomFlat), (ii) an homogeneous elastic medium with the real topography of Mt Etna (HomTop), (iii) an elastic heterogeneous medium with a flat surface (HetFlat), (iv) an elastic heterogeneous medium with the real topography (HetTop).

To better appraise such perturbations, we evaluated the displacement field at the GPS continuously running stations. Figure shows the horizontal GPS component together with results achieved by HomFlat, HomTop, HetFlat, HetTop numerical models. Discrepancies of few centimeters among analytical and numerical models are mainly restricted to the volcano summit area because of the accentuated topography and the medium heterogeneity.



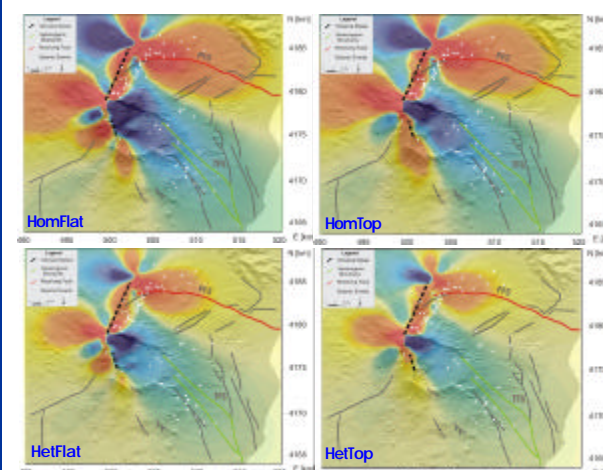
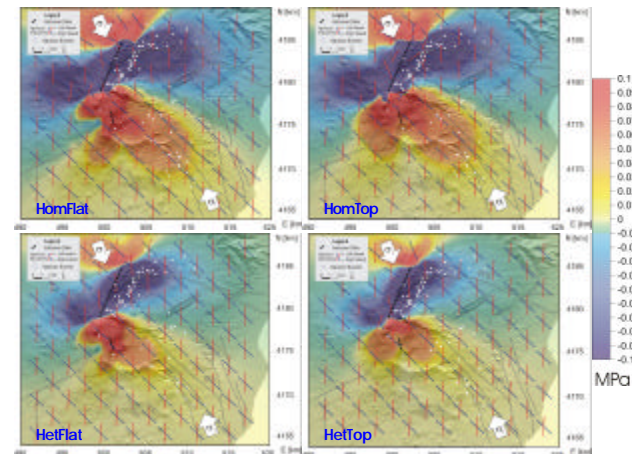
topography. The positive stress change in the north-eastern point out that the vertical uprising dike in the southern flank of the volcano generated an extensional stress field which promoted the lateral intrusion propagating along the pre-existing crustal fracture system of the NERift.

## Stress Changes on Rift North

To better understand the interaction between tectonic and intrusive processes, we firstly examined the stress transfer associated with the South dyke intrusion onto the North East Rift. The horizontal normal stress on the NERift is shown on a map view computed at 1 km bsl. Besides the amplitude and the shape of stress patterns, all the numerical models show a positive stress changes. The HomTop and HetTop numerical models show how the stress pattern is affected by the Mt Etna

## Stress Changes on Pernicana Fault and Timpe Fault System

We computed the induced stress by means of Coulomb failure stress changes defined by:  $\Delta CFF = \Delta\tau + \mu(\Delta\sigma_n + \Delta P)$  where  $\Delta\tau$  is the shear stress in the direction of slip on the receiver fault,  $\Delta\sigma_n$  is the normal stress change,  $\mu$  is the friction coefficient and  $\Delta P$  is the pore pressure change. The change in pore pressure is given as:  $\Delta P = -B \frac{\Delta\sigma_n}{3}$  where  $\Delta\sigma_n$  is the volumetric stress and  $B$  is the Skempton coefficient. We resolved the stress tensor generated by both the southern and northern dike intrusions onto the optimally oriented strike-slip faults and mapped structural trends of the Pernicana Fault (PF) and Timpe Fault System (TFS). We computed the optimally oriented plane (OOP) following King et al. (1994). Using as a reference regional stress field a horizontal  $\sigma_1$  oriented N337°, we obtain an OOP with orientations ranging from N340° to N20° for a left-lateral strike-slip fault and N110° to N157° for a right-lateral strike-slip fault.



The rupture along the TFS is optimally oriented while the PF is not optimally oriented. In such structurally complex areas, it is advisable to resolve directly the stress field onto the mapped structural trends. Therefore, we resolved the stress changes, generated by the southern and northern dike intrusions, onto a vertical plane oriented N100 with left lateral motion for the PF and onto a vertical plane oriented N145 with right lateral motion for the TFS. The maps emphasize the clear difference between the  $\Delta CFF$  resulting from resolving stress changes onto the Pernicana fault plane inferred from geological/structural constraints and that resulting from OOPs. The Coulomb stress change decreases from 0.8 MPa for the homogeneous models (HomFlat and HomTop) to 0.6 MPa for the heterogeneous model (HetFlat and HetTop), which gives a difference of 0.2 MPa in the most western part of the PF. The  $\Delta CFF$  resolved onto the TFS is quite similar to that resulting from OOPs; in all the numerical models, the TFS is encouraged to slip and it is optimally oriented.

